A DESIGN FRAMEWORK FOR TELEROBOTICS USING THE H_∞ APPROACH

T. I. Tsay
Mechanical Engineering Department
National Cheng Kung University
Tainan, Taiwan 70:01 ROC

H. Kazerooni
Mechanical Engineering Department
University of California at Berkeley
Berkeley, CA 94720 USA

Abstract[1]

This paper presents a design framework for a controller of a telerobotic system. The controller is designed so the dynamic behaviors of the master robot and the slave robot are functions of each other. This paper first describes these functions, which the designer sets based upon the application, and then proposes a control architecture to achieve these functions. To guarantee that the specified functions and proposed architecture govern the system behavior, H_∞ control theory and model reduction techniques are used. Several experiments were conducted to verify the theoretical derivations.

Nomenclature

All vectors are nx1 and all matrices are nxn, unless specified otherwise.

A_f :Matrix; desired force amplification
A_y :Matrix; desired position amplification
E :Matrix; environment impedance
e_f :Vector; deviation from the desired amplified force
e_y :Vector; deviation from the desired amplified position
e_{zm} :Vector; deviation from the desired master port impedance
e_{zs} :Vector; deviation from the desired slave port impedance
f_{ext} :Vector; any force imposed on the load other than slave robot
f_m :Vector; force imposed on the master robot by a human
f_s :Vector; force imposed on the slave robot by an environment[2]
G_m :Matrix; closed-loop position-tracking transfer function of a master robot
G_s :Matrix; closed-loop position-tracking transfer function of a slave robot
H :Matrix; controller
P :Introduced in Figure 3 and equation 9
S_h :Matrix; sensitivity of the human arm to the imposed motion
S_m :Matrix; sensitivity of the master robot with a closed-loop position controller to the imposed force
S_s :Matrix; sensitivity of the slave robot with a closed-loop position controller to the imposed force
u : $[u_m \ u_s]'$ (defined in equation 18)
u_h :vector; the human muscle force which initiates a maneuver
u_m :Vector; desired position of the master robot
u_s :Vector; desired position of the slave robot
v : $[u_h \ f_{ext}]'$ (defined in equation 18)
Wy :Matrix; weighting function, (equation 15)
Wf :Matrix; weighting function, (equation 16)
Wzm :Matrix; weighting function, (equation 17)
y : $[f_m \ f_s]'$ (defined in equation 18)
y_m :Vector; position of the master robot
y_s :Vector; position of the slave robot
z_m :Matrix; desired port impedance of the master robot
z_s :Matrix; desired port impedance of the slave robot

[1] This research work is supported by an NSF grant under IRI-9103955.
[2] In this paper, the word *environment* represents any object being manipulated or pushed by the slave robot.

1. Telerobotic Performance Specifications

A telerobotic system (Figure 1) consists of a master robot and a slave robot. For the telerobotic system, the designer can specify the desired behavior [2,13]. For example, the designer may want a dynamic behavior in which the human operator senses scaled-down values of the forces which the slave robot senses when maneuvering an object. To achieve this, a controller must be designed so the ratio of the forces on the slave, f_s, to the forces on the master, f_m, equals a number greater than unity. Then the desired relationship is $f_s = -\alpha f_m$, where α is a scalar greater than unity. (The negative sign, originating from the convention used in Figure 1, implies the opposite directions of f_s and f_m.) In another example, the slave is attached to a pneumatic jackhammer. Then, the objective may be both to attenuate and to filter the jackhammer forces so the human operator senses only low-frequency scaled-down components of the forces that the slave senses. This requires a low-pass filter-equivalent relationship, $f_m = \alpha f_s$, where α is a low-pass filter transfer function. In another example, instead of shaping the forces as in the examples above, it may be desirable to specify a desired relationship between the master and slave positions. For instance, the slave position could be a scaled-down version of the master position in order to have greater precision in maneuvering.

In general, it is desirable to shape the relationships between forces and positions at both ends of the telerobotic system. Inspection of Figure 1 reveals the relationships between the master and slave variables which have physical significance, that is f_m, y_m, f_s, and y_s,

$$y_s = A_y \, y_m \tag{1}$$

$$f_s = A_f \, f_m \tag{2}$$

$$f_m = Z_m \, y_m \tag{3}$$

$$f_s = Z_s \, y_s \tag{4}$$

Generally, A_y, A_f, Z_m, and Z_s are frequency-dependent matrices. A_y and A_f specify the amplification of position and force respectively between the master and the slave. Z_m and Z_s characterize the impedances of the master and slave ports. Since the four relationships are interdependent, the entire system performance is specfied when any three of these four relationships are specified. The next section introduces a practical control structure which achieves the performance specified by the four equations.

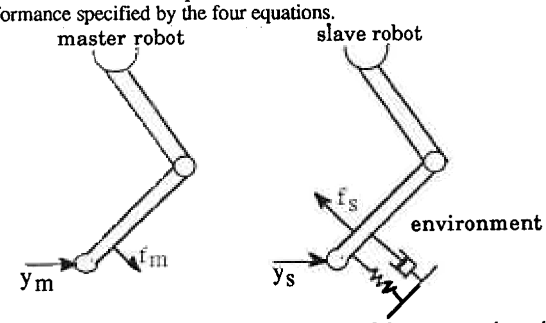

Figure 1: The human constrains the motion of the master robot while the environment constrains the motion of the slave robot.

2. The Control Architecture

Design of the control architecture must consider the dynamic behaviors of the master robot, the slave robot, the human operator, and the environment. These are discussed first.

Dynamic Behaviors of the Master Robot and the Slave Robot

It is assumed that both the master robot and the slave robot have independent closed-loop position controllers. For brevity, the selection of this controller is not discussed here. See Reference [1] for detailed description of such control method. The use of these primary stabilizing controllers in both the master robot and the slave robot is motivated by the following reasons.

1) For the safety of the human operator, the master must remain stable when not held by a human operator. A closed-loop position controller keeps the master robot stationary when not held by the operator.
2) For the security of the environment, the slave robot must remain stable if the communication between the slave and master is cut off accidentally. A closed-loop position controller keeps the slave robot stationary in these cases.
3) To attenuate the effects of nonlinear dynamics, a primary stabilizing compensator can eliminate the effects of friction force in its joints and transmission mechanism.

The derivations of the dynamic behaviors of the master robot and the slave robot are very similar, so only the master robot's dynamic behavior is derived here. The master robot's position, y_m, results from two inputs: u_m, the desired-position command to the master's position controller, and f_m, the forces imposed on the master robot. G_m is the primary closed-loop transfer function whose input is the desired-position command, u_m, and whose output is the master position, y_m. S_m is the "sensitivity" transfer function whose input is the force imposed on the master, f_m, and whose output is the master position, y_m. Thus, equation 5 represents the dynamic behavior of the master robot.

$$y_m = G_m \; u_m + S_m \; f_m \tag{5}$$

f_m represents force from only the human operator, since the master robot is in contact with only the human operator. The master robot has a small response to the human force, f_m, if the magnitude of S_m is small. A small S_m is achieved through the use of a high-gain closed-loop position controller as the primary controller or through the use of an actuator with a large gear ratio [8].

The dynamic behavior of the slave robot is defined by equation 6, which is similar to equation 5.

$$y_s = G_s \; u_s + S_s \; f_s \tag{6}$$

u_s is the desired position command to the slave position controller, and f_s is the force imposed on the slave robot endpoint by the environment. G_s and S_s are similar to G_m and S_m and represent the effects of u_s and f_s on y_s.

Dynamic Behavior of the Human Arm

The dynamic behavior of the human arm is modeled as a functional relationship between a set of inputs and a set of outputs. Therefore, the internal structure of the human operator is not of concern: the particular dynamics of nerve conduction, muscle contraction and central nervous system processing are implicitly accounted for in constructing the dynamic model of the human arm. Refer to [14] for a thorough review of various dynamic models of the human arm.

The force imposed by the human arm on the master robot results from two inputs. The first input, u_h, is the force imposed by the human muscles[3] and the second input, y_s, is the position of the slave robot. Thus, one may think of the master robot position as being a position disturbance occurring on the force-controlled human arm. If the master robot is stationary, the force imposed on the master robot is a function only of human muscle forces. However, if the master robot moves, the force imposed on the master robot is a function not only of the muscle forces but also of the master robot position. In other words, the human contact force with the master robot is disturbed and is different from u_h if the master robot is in motion. S_h maps the master robot position, y_m, onto the contact force, f_m, in equation 7.

$$f_m = u_h - S_h \, y_m \tag{7}$$

S_h is the human arm impedance and is determined primarily by the physical properties of the human arm.

Dynamic Behavior of the Environment

Telerobotic systems are used for manipulating objects or imposing force on objects. Defining E as a transfer function representing the dynamics of the environment and f_{ext} as the equivalent of all the external forces imposed on the environment, equation 8 provides a general expression for the force imposed on the slave robot in the linear domain.

$$f_s = -E \; y_s + f_{ext} \tag{8}$$

If the slave robot is used to push a spring and damper as shown in Figure 1, E is a transfer function so $E(s) = (k + c\,s)$ and $f_{ext} = 0$ where k, c and s are the stiffness, damping and Laplace operator, respectively.

The proposed control structure is shown in Figure 2, which also represents the dynamic behaviors of the telerobotic system, the human arm and the environment. Each dashed block represents one of the dynamic model equations 5 through 8. The information signals (the contact forces: f_m and f_s) are processed by controller H. The output of this controller is then fed to both drive systems, that of the master robot and that of the slave robot. Note that there is no position cross-feedback between the robots; only the contact forces are measured for feedback. This is a fundamental difference between this control structure and previous ones. (Refer to [6] and [7] for a summary of previous telerobotic control structures.) The motion of the master robot is partially due to the transfer of human power and partially due to the command generated by the computer. Since the mapping $G_m H_{11}$ acts in parallel to S_m, H_{11} has the effect of increasing the apparent sensitivity of the master robot. Similarly, compensator H_{22} is chosen to generate compliancy in the slave robot in response to the force f_s imposed on the endpoint of the slave robot [9, 11, 15]. The interaction force f_s also affects the master robot as a force reflection after passing through the the compensator H_{12}.

The goal of this effort is to find H so the chosen performance specifications, given by equations 1 through 4 are achieved and the stability of the system shown in Figure 1 is guaranteed.

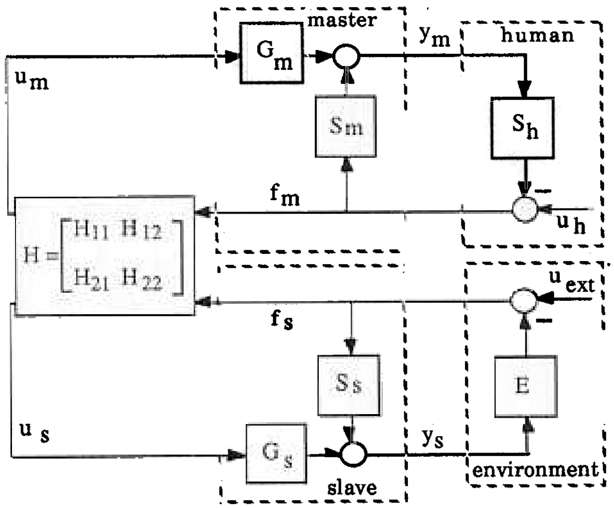

Figure 2: The proposed control structure.

[3]It is assumed that the specified form of u_h is not known other than that it is the result of human thought deciding to impose a force onto the master robot. The dynamic behavior in the generation of u_h by the human central nervous system is of little importance in this analysis since it does not affect the system performance and stability.

3. Review of the Standard H_∞ Control Problem

Figure 3 shows the basic block diagram used for the standard H_∞ control problem.

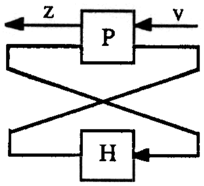

Figure 3: The standard H_∞ block diagram

In Figure 3, P is the generalized plant and H is the controller. P contains what is usually called the plant in a control system and also contains all weighting functions. The vector-valued signal v is the exogenous input, whose components are typically commands, disturbances and sensor noises. z is the output vector to be controlled, whose components are typically tracking errors. u is the control input vector. y is the measured output vector.

In order to express the closed-loop input-output mapping from v to z as a linear fractional transformation (LFT) on H, the interconnection structure P is partitioned in the following form:

$$P = \begin{bmatrix} P_{11} & P_{12} \\ P_{21} & P_{22} \end{bmatrix} \tag{9}$$

and: $z = P_{11}\, v + P_{12}\, u$ (10)

$y = P_{21}\, v + P_{22}\, u$ (11)

Then: $z = F\, v$ (12)

where: $F = P_{11} + P_{12}\, H\,(I - P_{22}\, H)^{-1}\, P_{21}$. (13)

The standard H_∞ control problem is to find a stabilizing controller H which minimizes $\| F \|_\infty$ (i.e., H_∞ norm of F), where:

$$\| C \|_\infty = \sup_\omega \bar{\sigma}\,(\, \| C \|_\infty (j\omega)\,) \tag{14}$$

$\bar{\sigma}(\cdot)$ denotes the maximum singular value. A detailed review of H_∞ is given in [4] and state-space results are discussed in [3]. In this algorithm H_∞ norm minimization is used to obtain a stabilizing controller H so $\| F_1 \|_\infty < \gamma$, where γ is a positive small number and may be interpreted as a measure of performance.

4. Problem Formulation

Depending on the application, the designer is free to choose any three of the four relationships in equations 1 through 4 to specify the system performance. This article chooses Ay, A_f and Z_m (i.e., equations 1, 2 and 3) as the performance specifications for the example solution herein. (The solution obtained in this article can be achieved similarly for all other possible combinations.) Now having fixed the performance specifications, the control problem reduces to designing a controller that guarantees minimal deviations of the system performance from the chosen performance specifications. Equations 15, 16 and 17 represent possible deviations in the system performance.

$$z_1 = W_y\,(y_s - A_y\, y_m) \tag{15}$$

$$z_2 = W_f\,(f_s - A_f\, f_m) \tag{16}$$

$$z_3 = W_{zm}\,(y_m - Z_m^{-1}\, f_m) \tag{17}$$

where Wy, W_f and W_{zm} are weighting function matrices. The block diagram of Figure 4 is derived from Figure 2 to represent z_1, z_2, z_3. This block diagram is converted to the architecture of Figure 3 by choosing:

$$z = \begin{bmatrix} z_1 \\ z_2 \\ z_3 \end{bmatrix},\quad v = \begin{bmatrix} u_h \\ f_{ext} \end{bmatrix},\quad y = \begin{bmatrix} f_m \\ f_s \end{bmatrix},\quad u = \begin{bmatrix} u_m \\ u_s \end{bmatrix},\quad H = \begin{bmatrix} H_{11} & H_{12} \\ H_{21} & H_{22} \end{bmatrix} \tag{18}$$

$$P_{11} = \begin{bmatrix} -W_yA_yS_m(I+S_hS_m)^{-1} & W_yS_s(I+ES_s)^{-1} \\ -W_fA_f(I+S_hS_m)^{-1} & W_f(I+ES_s)^{-1} \\ W_{zm}(S_m-Z_m^{-1})(I+S_hS_m)^{-} & 0 \end{bmatrix} \tag{19}$$

$$P_{12} = \begin{bmatrix} -W_yA_yS_h^{-1}(I+S_hS_m)^{-1}S_hG_m & W_yS_s(I+ES_s)^{-1}S_s^{-1}G_s \\ W_fA_f(I+S_hS_m)^{-1}S_hG_m & -W_f(I+ES_s)^{-1}EG_s \\ W_{zm}(S_h^{-1}+Z_m^{-1})(I+S_hS_m)^{-1}S_hG_m & 0 \end{bmatrix} \tag{20}$$

$$P_{21} = \begin{bmatrix} (I+S_hS_m)^{-1} & 0 \\ 0 & (I+ES_s)^{-1} \end{bmatrix} \tag{21}$$

$$P_{22} = \begin{bmatrix} -(I+S_hS_m)^{-1}S_hG_m & 0 \\ 0 & -(I+ES_s)^{-1}EG_s \end{bmatrix} \tag{22}$$

An internally balanced realization [5, 12] is performed to find matrix H so minimizes $\| F \|_\infty$ is minimized where F maps v to z as in equation 12. The order of the resulting controller is high. A reduced-order controller is obtained by neglecting the weakly controllable and observable states of the controller.

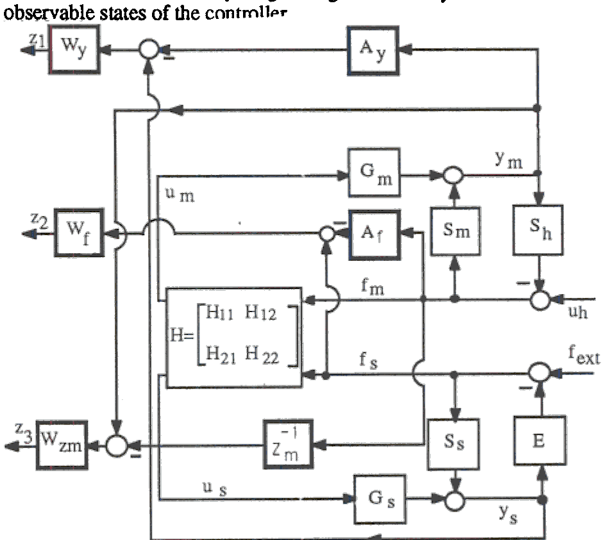

Figure 4: The control problem is to find a stabilizing controller H which minimizes z.

5. Experiments

Figure 5 shows the experimental setup: a two-degree-of-freedom X-Y table used as the master robot. A three-degree-of-freedom composite robot [10] is used as the slave robot. Since the master robot operates only on a horizontal plane, one of the slave's robot actuators is physically locked so that the slave robot operates only on the horizontal plane also. The human operator holds a handle to move the master robot. f_m, the contact force between the operator and master robot, is measured by a force sensor on the handle. f_s, the contact force between the slave robot and the environment, is measured by a force sensor at the slave robot endpoint.

Robot Dynamics

The primary stabilizing controller for the master robot is a lead-lag controller. This controller achieves the widest bandwidth for the closed-loop position transfer function matrix G_m, and yet stabilizes the X-Y table in the presence of unmodeled dynamics. Since the table motion is uncoupled, G_m is a 2x2 diagonal transfer function matrix representing the X-Y table dynamics in the X-direction and Y-direction (Figure 6). The analytical form of G_m was verified experimentally via a frequency response method and is given by equation 23.

$$G_m = \begin{bmatrix} \dfrac{1}{\left(\dfrac{s^2}{31^2} + \dfrac{s}{25} + 1\right)} & 0 \\ 0 & \dfrac{1}{\left(\dfrac{s^2}{12.2^2} + \dfrac{s}{13.4} + 1\right)} \end{bmatrix} \text{cm/cm} \quad (23)$$

Due to the low pitch angle of the lead-screw mechanism, the X-Y table is not backdrivable. Therefore, the master robot cannot be moved by the force exerted on the handle by the human operator, and S_m is virtually equal to zero.

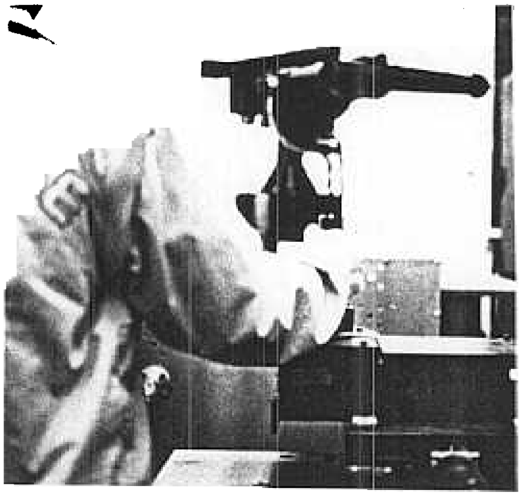

Figure 5: A photograph of the experimental setup.

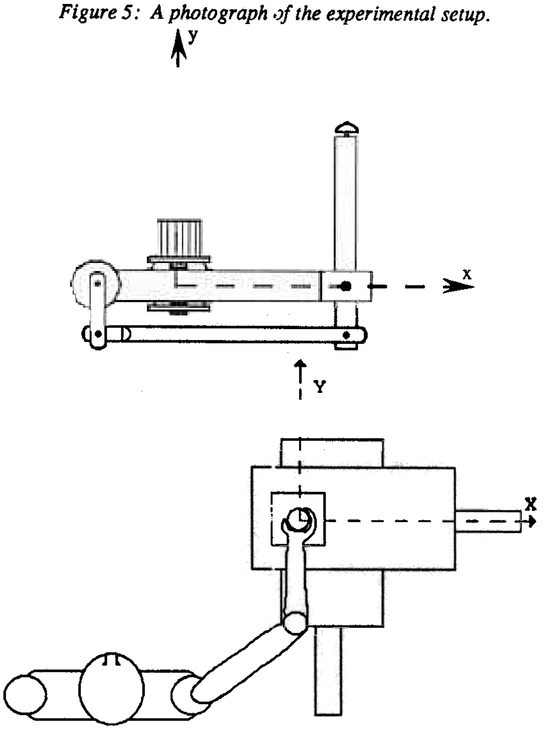

Figure 6: A top view of the master and slave robot

A computed torque method and a PD controller were used as the primary stabilizing controller for the slave robot. This controller develops an uncoupled dynamic model for the robot. The resulting approximate closed-loop transfer function matrix and sensitivity matrix are as follows.

$$G_s = \begin{bmatrix} \dfrac{1690.9}{s^2 + 42.1\,s + 1690.9} & 0 \\ 0 & \dfrac{1503.6}{s^2 + 40.3\,s + 1503.6} \end{bmatrix} \text{cm/cm} \quad (24)$$

$$S_s = \begin{bmatrix} \dfrac{89.19}{s^2 + 39.80\,s + 531.54} & 0 \\ 0 & \dfrac{12.08}{s^2 + 36.76\,s + 483.79} \end{bmatrix} \text{cm/N} \quad (25)$$

Human Arm Dynamics

The human arm model derived here does not represent the human arm sensitivity, S_h, for all configurations, but is only an approximate and experimentally verified dynamic model of the author's arm in the neighborhood of the operating configuration shown in Figure 6. In the identifying process, the operator was seated next to the master robot while grasping the handle with his right hand as shown in Figure 6. The master robot was commanded to oscillate in a sinusoidal fashion along the x and y axes respectively. At each oscillation frequency, the operator attempted to move his arm to follow the master robot so that no contact force between his hand and the master robot was generated (i.e., he decided not to impose any force on the master robot ($u_h = 0$)). Since the human arm cannot keep up with any high frequency movement of the master when trying to maintain zero contact force, a large contact force and consequently a large S_h are expected at high frequencies. Since this force is equal to the product of the master acceleration and the human arm inertia (Newton's Second Law), at least a second-order transfer function is expected at high frequencies. At low frequencies, however, the human can follow the large motions of the master robot quite comfortably, but it is expected that some finite contact force is present. Therefore, the human arm sensitivity approaches a finite value at low frequencies. Based upon the experimental data, the best estimates for the author's arm sensitivities along the x and y axes are:

$$S_h = \begin{bmatrix} 0.15\left(\dfrac{s^2}{3.2^2} + \dfrac{s}{2.5} + 1\right) & 0 \\ 0 & 0.13\left(\dfrac{s^2}{2.75^2} + \dfrac{s}{2.15} + 1\right) \end{bmatrix} \text{N/cm} \quad (26)$$

Environment Dynamics

Figure 7 shows the environment simulator. This simulator consists of two metal boards. Compression-type helical springs are positioned between the stationary and movable metal boards to furnish resistive force between the plates. The stationary board is mounted tight. The dynamic model of the movable plate is expressed by equation 27.

$$E = 21.582 \quad \text{N/cm} \quad (27)$$

where E us defined by equation 8.

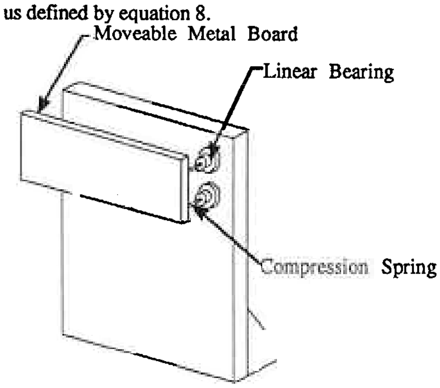

Figure 7: The schematic of the experiment simulator.

The environment simulator was set at a 10^o angle with the Cartesian coordinate x-axis as shown in Figure 7. The chosen performance specifications for A_f and Z_m are given by the following equations.

$$A_f = \begin{bmatrix} A_{f_x} & 0 \\ 0 & A_{f_y} \end{bmatrix} \quad (28)$$

$$Z_m = \begin{bmatrix} Z_{m_x} & 0 \\ 0 & Z_{m_y} \end{bmatrix} \quad (29)$$

where: $Z_{mx} = Z_{my} = 4\,s + 0.04$ N/cm (30)

and $A_{fx} = -0.5$ and $A_{fy} = -1.5$ (31)

The elements of all weighting functions were chosen as $\frac{0.01}{s+1}$. Through the controller design procedure given in section 3, the controller was designed. Figures 8 shows the slave force and the master force along the X-direction. Figure 9 shows the slave force versus the master force where the slope of the fitted curve confirms the achievement of the desired force attenuation in the X-direction. Figures 10 and 11 are similar to figures 8 and 9 and show the force amplification along the Y-direction.

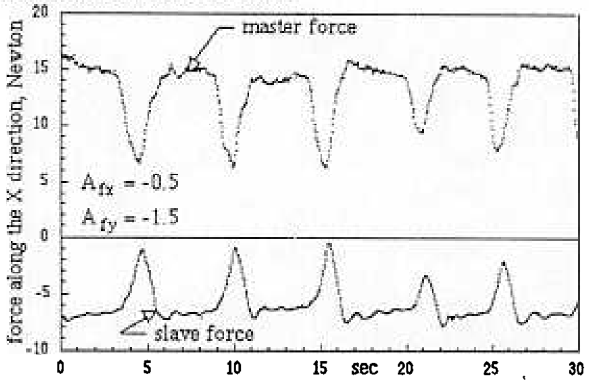

Figure 8: Plots of master and slave forces along the x-direction.

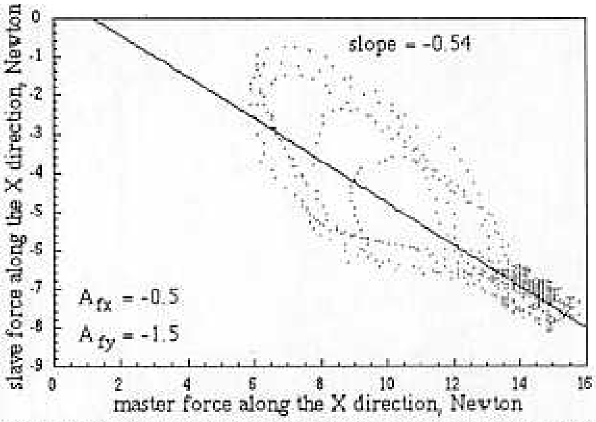

Figure 9: The slope of the fitted linear curve = - 0.54 confirms the force amplification of A_{fx} = - 0.5 along the x direction.

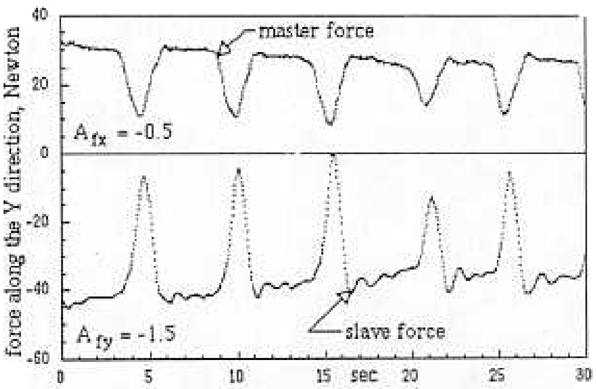

Figure 10: Plots of master and slave forces along the Y-direction

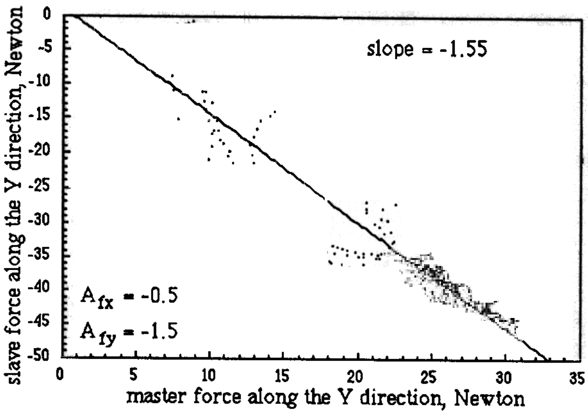

Figure 11: The slope of the fitted linear curve = - 1.55 confirms the force amplification of A_{fy} = - 1.5 along the y direction.

6. Summary and Conclusion

This paper presents a design framework for telerobotic systems to achieve desired dynamic relationships between the master robot and the slave robot. H_∞ control theory and model reduction techniques were used to guarantee that the system behavior was governed by the proposed specified functions. Several experiments were carried out to verify the theoretical derivations

7. References

1) Anderson, R. J., Spong, M. W., "Asymptotic Stability for Force Reflecting Teleoperators with Time Delay", IEEE Int. Conf. on Robotics and Automation, Scottsdale, AZ, May 1989.
2) Bejczy, A. K., Bekey, G., Lee, S. K., "Computer Control of Space Borne Teleoperators with Sensory Feedback", IEEE Conference on Robotics and Automation, 1985.
3) Doyle, J. C., Glover, K., Khargonekar, P., Francis, B. A., "State-Space Solutions to Standard H_2 and H_∞ Control Problems", IEEE Trans. on Aut. Control, V. 34. No. 8, 1989.
4) Francis, Bruce A., A Course in H_∞ Control Theory, Springer-Verlag, Berlin, 1987.
5) Glover, K.,"All Optimal Hankel-norm Approximations of Linear Multivariable Systems and Their L_∞ Error Bounds", International Journal of Control, Vol. 39, pp. 1115-1193, 1984.
6) Hannaford, B., "A Design Framework for Teleoperators with Kinematic Feedback", IEEE Transactions on Robotics and Automation, Vol. 5, No. 4, Aug. 1989.
7) Hannaford, B., "Stability and Performance Tradeoff in Bilateral Telemanipulations", IEEE Int. Conference on Robotics and Automation, Scottsdale, AZ, May 1989.
8) Kazerooni, H., "On the Robot Compliant Motion Control", ASME J. of Dyn. Systems, Measurement, and Control, Vol. 111, No. 3, Sep. 1989.
9) Kazerooni, H., Houpt, P. K., Sheridan, T. B., "Fundamentals of Robust Compliant Motion for Manipulators", IEEE Journal of Robotics and Automation, Vo'. 2, No. 2, Jun. 1986.
10) Kazerooni H., Kim S., "On the Design of Direct Drive Robots," ASME Journal of Engineering for Industry. Vol. 112, No. 2, May 1990.
11) Kazerooni, H., "On the Contact Instability of the Robots When Constrained by Rigid Environments," IEEE Transactions on Automatic Control, Volume 35, Number 6, June 1990.
12) Moore, B. C., "Principal Component Analysis in Linear System: Controllability, Observability and Model Reduction", IEEE Transactions on Automatic Control, AC-26, Feb. 1981.
13) Raju, G. J., Verghese, G. C., Sheridan, T. B., "Design Issues in Network Models of Bilateral Remote Manipulation", IEEE Int. Conf. on Robotics and Aut., Scottsdale, AZ, May 1989.
14) Stein, R. B., "What muscles variables does the nervous system control in limb movements?", J. of the Behavioral and Brain Sciences, Vol. 5, pp. 535-577, 1982.
15) Waibel, B. J., Kazerooni, H., "On the Stability of the Constrained Robotic Maneuvers in the Presence of Modeling Uncertainties," IEEE Transaction on Robotics and Automation, Vol. 7 No. 1. February 1991.

A DESIGN FRAMEWORK FOR TELEROBOTICS USING THE H_∞ APPROACH

T. I. Tsay
Mechanical Engineering Department
National Cheng Kung University
Tainan, Taiwan 70101 ROC

H. Kazerooni
Mechanical Engineering Department
University of California at Berkeley
Berkeley, CA 94720 USA

Abstract[1]

This paper presents a design framework for a controller of a telerobotic system. The controller is designed so the dynamic behaviors of the master robot and the slave robot are functions of each other. This paper first describes these functions, which the designer sets based upon the application, and then proposes a control architecture to achieve these functions. To guarantee that the specified functions and proposed architecture govern the system behavior, H_∞ control theory and model reduction techniques are used. Several experiments were conducted to verify the theoretical derivations.

Nomenclature

All vectors are nx1 and all matrices are nxn, unless specified otherwise.

A_f	:Matrix; desired force amplification
A_y	:Matrix; desired position amplification
E	:Matrix; environment impedance
e_f	:Vector; deviation from the desired amplified force
e_y	:Vector; deviation from the desired amplified position
e_{zm}	:Vector; deviation from the desired master port impedance
e_{zs}	:Vector; deviation from the desired slave port impedance
f_{ext}	:Vector; any force imposed on the load other than slave robot
f_m	:Vector; force imposed on the master robot by a human
f_s	:Vector; force imposed on the slave robot by an environment[2]
G_m	:Matrix; closed-loop position-tracking transfer function of a master robot
G_s	:Matrix; closed-loop position-tracking transfer function of a slave robot
H	:Matrix; controller
P	:Introduced in Figure 3 and equation 9
S_h	:Matrix; sensitivity of the human arm to the imposed motion
S_m	:Matrix; sensitivity of the master robot with a closed-loop position controller to the imposed force
S_s	:Matrix; sensitivity of the slave robot with a closed-loop position controller to the imposed force
u	: $[u_m \; u_s]'$ (defined in equation 18)
u_h	:vector; the human muscle force which initiates a maneuver
u_m	:Vector; desired position of the master robot
u_s	:Vector; desired position of the slave robot
v	: $[u_h \; f_{ext}]'$ (defined in equation 18)
Wy	:Matrix; weighting function, (equation 15)
Wf	:Matrix; weighting function, (equation 16)
Wzm	:Matrix; weighting function, (equation 17)
y	: $[f_m \; f_s]'$ (defined in equation 18)
y_m	:Vector; position of the master robot
y_s	:Vector; position of the slave robot
z_m	:Matrix; desired port impedance of the master robot
z_s	:Matrix; desired port impedance of the slave robot

[1] This research work is supported by an NSF grant under IRI-9103955.

[2] In this paper, the word *environment* represents any object being manipulated or pushed by the slave robot.

1. Telerobotic Performance Specifications

A telerobotic system (Figure 1) consists of a master robot and a slave robot. For the telerobotic system, the designer can specify the desired behavior [2,13]. For example, the designer may want a dynamic behavior in which the human operator senses scaled-down values of the forces which the slave robot senses when maneuvering an object. To achieve this, a controller must be designed so the ratio of the forces on the slave, f_s, to the forces on the master, f_m, equals a number greater than unity. Then the desired relationship is $f_s = -\alpha f_m$, where α is a scalar greater than unity. (The negative sign, originating from the convention used in Figure 1, implies the opposite directions of f_s and f_m.) In another example, the slave is attached to a pneumatic jackhammer. Then, the objective may be both to attenuate and to filter the jackhammer forces so the human operator senses only low-frequency scaled-down components of the forces that the slave senses. This requires a low-pass filter-equivalent relationship, $f_m = \alpha f_s$, where α is a low-pass filter transfer function. In another example, instead of shaping the forces as in the examples above, it may be desirable to specify a desired relationship between the master and slave positions. For instance, the slave position could be a scaled-down version of the master position in order to have greater precision in maneuvering.

In general, it is desirable to shape the relationships between forces and positions at both ends of the telerobotic system. Inspection of Figure 1 reveals the relationships between the master and slave variables which have physical significance, that is f_m, y_m, f_s, and y_s,

$$y_s = A_y \; y_m \qquad (1)$$

$$f_s = A_f \; f_m \qquad (2)$$

$$f_m = Z_m \; y_m \qquad (3)$$

$$f_s = Z_s \; y_s \qquad (4)$$

Generally, A_y, A_f, Z_m, and Z_s are frequency-dependent matrices. A_y and A_f specify the amplification of position and force respectively between the master and the slave. Z_m and Z_s characterize the impedances of the master and slave ports. Since the four relationships are interdependent, the entire system performance is specfied when any three of these four relationships are specified. The next section introduces a practical control structure which achieves the performance specified by the four equations.

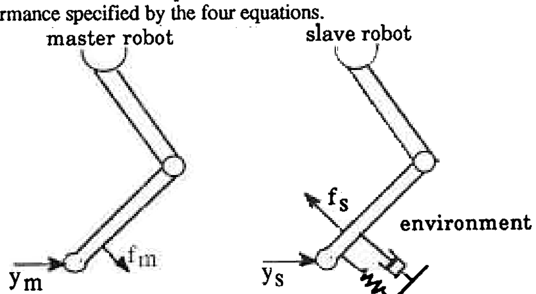

Figure 1: The human constrains the motion of the master robot while the environment constrains the motion of the slave robot.

2. The Control Architecture

Design of the control architecture must consider the dynamic behaviors of the master robot, the slave robot, the human operator, and the environment. These are discussed first.

Dynamic Behaviors of the Master Robot and the Slave Robot

It is assumed that both the master robot and the slave robot have independent closed-loop position controllers. For brevity, the selection of this controller is not discussed here. See Reference [1] for detailed description of such control method. The use of these primary stabilizing controllers in both the master robot and the slave robot is motivated by the following reasons.

1) For the safety of the human operator, the master must remain stable when not held by a human operator. A closed-loop position controller keeps the master robot stationary when not held by the operator.
2) For the security of the environment, the slave robot must remain stable if the communication between the slave and master is cut off accidentally. A closed-loop position controller keeps the slave robot stationary in these cases.
3) To attenuate the effects of nonlinear dynamics, a primary stabilizing compensator can eliminate the effects of friction force in its joints and transmission mechanism.

The derivations of the dynamic behaviors of the master robot and the slave robot are very similar, so only the master robot's dynamic behavior is derived here. The master robot's position, y_m, results from two inputs: u_m, the desired-position command to the master's position controller, and f_m, the forces imposed on the master robot. G_m is the primary closed-loop transfer function whose input is the desired-position command, u_m, and whose output is the master position, y_m. S_m is the "sensitivity" transfer function whose input is the force imposed on the master, f_m, and whose output is the master position, y_m. Thus, equation 5 represents the dynamic behavior of the master robot.

$$y_m = G_m u_m + S_m f_m \tag{5}$$

f_m represents force from only the human operator, since the master robot is in contact with only the human operator. The master robot has a small response to the human force, f_m, if the magnitude of S_m is small. A small S_m is achieved through the use of a high-gain closed-loop position controller as the primary controller or through the use of an actuator with a large gear ratio [8].

The dynamic behavior of the slave robot is defined by equation 6, which is similar to equation 5.

$$y_s = G_s u_s + S_s f_s \tag{6}$$

u_s is the desired position command to the slave position controller, and f_s is the force imposed on the slave robot endpoint by the environment. G_s and S_s are similar to G_m and S_m and represent the effects of u_s and f_s on y_s.

Dynamic Behavior of the Human Arm

The dynamic behavior of the human arm is modeled as a functional relationship between a set of inputs and a set of outputs. Therefore, the internal structure of the human operator is not of concern: the particular dynamics of nerve conduction, muscle contraction and central nervous system processing are implicitly accounted for in constructing the dynamic model of the human arm. Refer to [14] for a thorough review of various dynamic models of the human arm.

The force imposed by the human arm on the master robot results from two inputs. The first input, u_h, is the force imposed by the human muscles[3] and the second input, y_s, is the position of the slave robot. Thus, one may think of the master robot position as being a position disturbance occurring on the force-controlled human arm. If the master robot is stationary, the force imposed on the master robot is a function only of human muscle forces. However, if the master robot moves, the force imposed on the master robot is a function not only of the muscle forces but also of the master robot position. In other words, the human contact force with the master robot is disturbed and is different from u_h if the master robot is in motion. S_h maps the master robot position, y_m, onto the contact force, f_m, in equation 7.

$$f_m = u_h - S_h y_m \tag{7}$$

S_h is the human arm impedance and is determined primarily by the physical properties of the human arm.

Dynamic Behavior of the Environment

Telerobotic systems are used for manipulating objects or imposing force on objects. Defining E as a transfer function representing the dynamics of the environment and f_{ext} as the equivalent of all the external forces imposed on the environment, equation 8 provides a general expression for the force imposed on the slave robot in the linear domain.

$$f_s = -E\, y_s + f_{ext} \tag{8}$$

If the slave robot is used to push a spring and damper as shown in Figure 1, E is a transfer function so $E(s) = (k + c\,s)$ and $f_{ext} = 0$ where k, c and s are the stiffness, damping and Laplace operator, respectively.

The proposed control structure is shown in Figure 2, which also represents the dynamic behaviors of the telerobotic system, the human arm and the environment. Each dashed block represents one of the dynamic model equations 5 through 8. The information signals (the contact forces: f_m and f_s) are processed by controller H. The output of this controller is then fed to both drive systems, that of the master robot and that of the slave robot. Note that there is no position cross-feedback between the robots; only the contact forces are measured for feedback. This is a fundamental difference between this control structure and previous ones. (Refer to [6] and [7] for a summary of previous telerobotic control structures.) The motion of the master robot is partially due to the transfer of human power and partially due to the command generated by the computer. Since the mapping $G_m H_{11}$ acts in parallel to S_m, H_{11} has the effect of increasing the apparent sensitivity of the master robot. Similarly, compensator H_{22} is chosen to generate compliancy in the slave robot in response to the force f_s imposed on the endpoint of the slave robot [9, 11, 15]. The interaction force f_s also affects the master robot as a force reflection after passing through the the compensator H_{12}.

The goal of this effort is to find H so the chosen performance specifications, given by equations 1 through 4 are achieved and the stability of the system shown in Figure 1 is guaranteed.

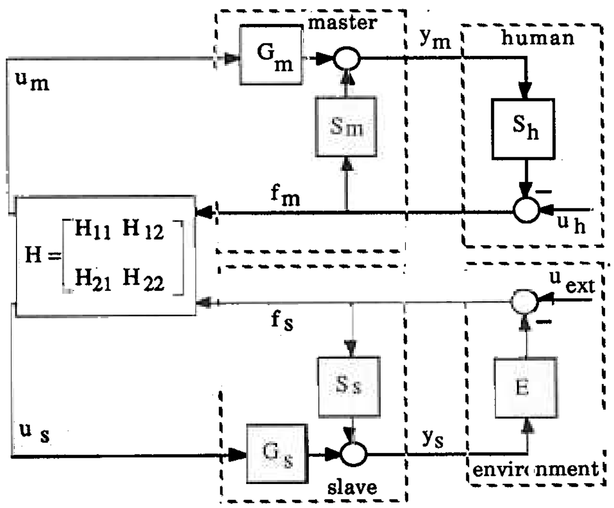

Figure 2: The proposed control structure.

[3] It is assumed that the specified form of u_h is not known other than that it is the result of human thought deciding to impose a force onto the master robot. The dynamic behavior in the generation of u_h by the human central nervous system is of little importance in this analysis since it does not affect the system performance and stability.

3. Review of the Standard H_∞ Control Problem

Figure 3 shows the basic block diagram used for the standard H_∞ control problem.

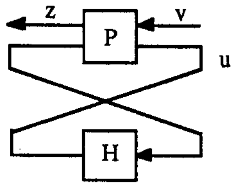

Figure 3: The standard H_∞ block diagram

In Figure 3, P is the generalized plant and H is the controller. P contains what is usually called the plant in a control system and also contains all weighting functions. The vector-valued signal v is the exogenous input, whose components are typically commands, disturbances and sensor noises. z is the output vector to be controlled, whose components are typically tracking errors. u is the control input vector. y is the measured output vector.

In order to express the closed-loop input-output mapping from v to z as a linear fractional transformation (LFT) on H, the interconnection structure P is partitioned in the following form:

$$P = \begin{bmatrix} P_{11} & P_{12} \\ P_{21} & P_{22} \end{bmatrix} \tag{9}$$

$$\text{and: } z = P_{11}\, v + P_{12}\, u \tag{10}$$

$$y = P_{21}\, v + P_{22}\, u \tag{11}$$

$$\text{Then: } z = F\, v \tag{12}$$

$$\text{where: } F = P_{11} + P_{12}\, H\,(I - P_{22}\, H)^{-1}\, P_{21}. \tag{13}$$

The standard H_∞ control problem is to find a stabilizing controller H which minimizes $\| F \|_\infty$ (i.e., H_∞ norm of F), where:

$$\| C \|_\infty = \sup_\omega \bar{\sigma}\, (\| C \|_\infty (j\omega)) \tag{14}$$

$\bar{\sigma}(\cdot)$ denotes the maximum singular value. A detailed review of H_∞ is given in [4] and state-space results are discussed in [3]. In this algorithm H_∞ norm minimization is used to obtain a stabilizing controller H so $\| F_1 \|_\infty < \gamma$, where γ is a positive small number and may be interpreted as a measure of performance.

4. Problem Formulation

Depending on the application, the designer is free to choose any three of the four relationships in equations 1 through 4 to specify the system performance. This article chooses Ay, A_f and Z_m (i.e., equations 1, 2 and 3) as the performance specifications for the example solution herein. (The solution obtained in this article can be achieved similarly for all other possible combinations.) Now having fixed the performance specifications, the control problem reduces to designing a controller that guarantees minimal deviations of the system performance from the chosen performance specifications. Equations 15, 16 and 17 represent possible deviations in the system performance.

$$z_1 = Wy\,(y_s - Ay\; y_m) \tag{15}$$

$$z_2 = W_f\,(f_s - A_f\; f_m) \tag{16}$$

$$z_3 = W_{zm}\,(y_m - Z_m^{-1}\; f_m) \tag{17}$$

where Wy, W_f and W_{zm} are weighting function matrices. The block diagram of Figure 4 is derived from Figure 2 to represent z_1, z_2, z_3. This block diagram is converted to the architecture of Figure 3 by choosing:

$$= \begin{bmatrix} z_1 \\ z_2 \\ z_3 \end{bmatrix},\; v = \begin{bmatrix} u_h \\ f_{ext} \end{bmatrix},\; y = \begin{bmatrix} f_m \\ f_s \end{bmatrix},\; u = \begin{bmatrix} u_m \\ u_s \end{bmatrix},\; H = \begin{bmatrix} H_{11} & H_{12} \\ H_{21} & H_{22} \end{bmatrix} \tag{18}$$

$$P_{11} = \begin{bmatrix} -WyAyS_m(I+S_hS_m)^{-1} & WyS_s(I+ES_s)^{-1} \\ -W_fA_f(I+S_hS_m)^{-1} & W_f(I+ES_s)^{-1} \\ W_{zm}(S_m-Z_m^{-1})(I+S_hS_m)^{-1} & 0 \end{bmatrix} \tag{19}$$

$$P_{12} = \begin{bmatrix} -WyAyS_h^{-1}(I+S_hS_m)^{-1}S_hG_m & WyS_s(I+ES_s)^{-1}S_s^{-1}G_s \\ W_fA_f(I+S_hS_m)^{-1}S_hG_m & -W_f(I+ES_s)^{-1}EG_s \\ W_{zm}(S_h^{-1}+Z_m^{-1})(I+S_hS_m)^{-1}S_hG_m & 0 \end{bmatrix} \tag{20}$$

$$P_{21} = \begin{bmatrix} (I+S_hS_m)^{-1} & 0 \\ 0 & (I+ES_s)^{-1} \end{bmatrix} \tag{21}$$

$$P_{22} = \begin{bmatrix} -(I+S_hS_m)^{-1}S_hG_m & 0 \\ 0 & -(I+ES_s)^{-1}EG_s \end{bmatrix} \tag{22}$$

An internally balanced realization [5, 12] is performed to find matrix H so minimizes $\| F \|_\infty$ is minimized where F maps v to z as in equation 12. The order of the resulting controller is high. A reduced-order controller is obtained by neglecting the weakly controllable and observable states of the controller.

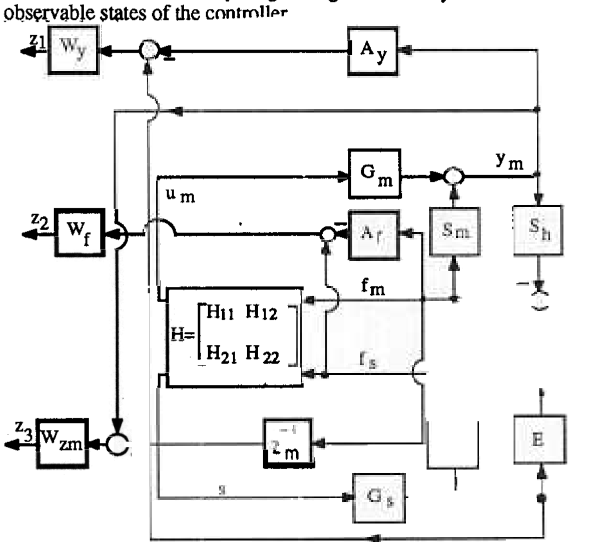

Figure 4: The control problem is to find a stabilizing controller H which minimizes z.

5. Experiments

Figure 5 shows the experimental setup: a two-degree-of-freedom X-Y table used as the master robot. A three-degree-of-freedom composite robot [10] is used as the slave robot. Since the master robot operates only on a horizontal plane, one of the slave's robot actuators is physically locked so that the slave robot operates only on the horizontal plane also. The human operator holds a handle to move the master robot. f_m, the contact force between the operator and master robot, is measured by a force sensor on the handle. f_s, the contact force between the slave robot and the environment, is measured by a force sensor at the slave robot endpoint.

Robot Dynamics

The primary stabilizing controller for the master robot is a lead-lag controller. This controller achieves the widest bandwidth for the closed-loop position transfer function matrix G_m, and yet stabilizes the X-Y table in the presence of unmodeled dynamics. Since the table motion is uncoupled, G_m is a 2x2 diagonal transfer function matrix representing the X-Y table dynamics in the X-direction and Y-direction (Figure 6). The analytical form of G_m was verified experimentally via a frequency response method and is given by equation 23.

$$G_m = \begin{bmatrix} \frac{1}{(\frac{s^2}{31^2} + \frac{s}{25} + 1)} & 0 \\ 0 & \frac{\quad}{(\frac{s^2}{12.2^2} + \frac{s}{13.4} + 1)} \end{bmatrix} \text{cm/cm} \quad (23)$$

Due to the low pitch angle of the lead-screw mechanism, the X-Y table is not backdrivable. Therefore, the master robot cannot be moved by the force exerted on the handle by the human operator, and S_m is virtually equal to zero.

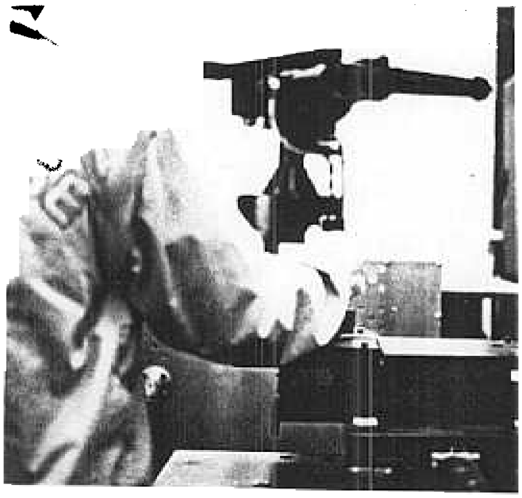

Figure 5: A photograph of the experimental setup.

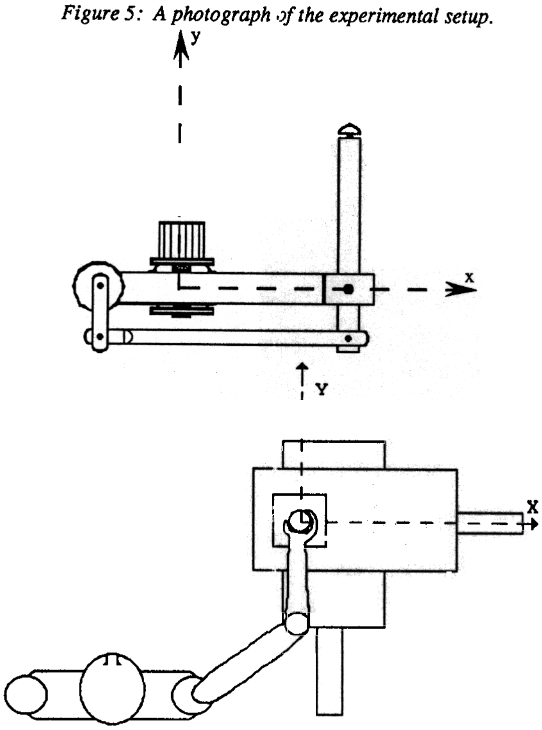

Figure 6: A top view of the master and slave robot

A computed torque method and a PD controller were used as the primary stabilizing controller for the slave robot. This controller develops an uncoupled dynamic model for the robot. The resulting approximate closed-loop transfer function matrix and sensitivity matrix are as follows.

$$G_s = \begin{bmatrix} \frac{1690.9}{s^2 + 42.1\, s + 1690.9} & 0 \\ 0 & \frac{1503.6}{s^2 + 40.3\, s + 1503.6} \end{bmatrix} \text{cm/cm} \quad (24)$$

$$S_s = \begin{bmatrix} \frac{89.19}{s^2 + 39.80\, s + 531.54} & 0 \\ 0 & \frac{12.08}{s^2 + 36.76\, s + 483.79} \end{bmatrix} \text{cm/N} \quad (25)$$

Human Arm Dynamics

The human arm model derived here does not represent the human arm sensitivity, S_h, for all configurations, but is only an approximate and experimentally verified dynamic model of the author's arm in the neighborhood of the operating configuration shown in Figure 6. In the identifying process, the operator was seated next to the master robot while grasping the handle with his right hand as shown in Figure 6. The master robot was commanded to oscillate in a sinusoidal fashion along the x and y axes respectively. At each oscillation frequency, the operator attempted to move his arm to follow the master robot so that no contact force between his hand and the master robot was generated (i.e., he decided not to impose any force on the master robot ($u_h = 0$)). Since the human arm cannot keep up with any high frequency movement of the master when trying to maintain zero contact force, a large contact force and consequently a large S_h are expected at high frequencies. Since this force is equal to the product of the master acceleration and the human arm inertia (Newton's Second Law), at least a second-order transfer function is expected at high frequencies. At low frequencies, however, the human can follow the large motions of the master robot quite comfortably, but it is expected that some finite contact force is present. Therefore, the human arm sensitivity approaches a finite value at low frequencies. Based upon the experimental data, the best estimates for the author's arm sensitivities along the x and y axes are:

$$S_h = \begin{bmatrix} 0.15\,(\frac{s^2}{3.2^2} + \frac{s}{2.5} + 1) & 0 \\ 0 & 0.13\,(\frac{s^2}{2.75^2} + \frac{s}{2.15} + 1) \end{bmatrix} \text{N/cm} \quad (26)$$

Environment Dynamics

Figure 7 shows the environment simulator. This simulator consists of two metal boards. Compression-type helical springs are positioned between the stationary and movable metal boards to furnish resistive force between the plates. The stationary board is mounted tight. The dynamic model of the movable plate is expressed by equation 27.

$$E = 21.582 \quad \text{N/cm} \quad (27)$$

where E us defined by equation 8.

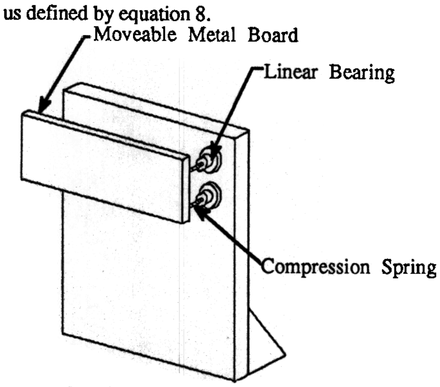

Figure 7: The schematic of the experiment simulator.

The environment simulator was set at a 10^o angle with the Cartesian coordinate x-axis as shown in Figure 7. The chosen performance specifications for A_f and Z_m are given by the following equations.

$$A_f = \begin{bmatrix} A_{fx} & 0 \\ 0 & A_{fy} \end{bmatrix} \quad (28)$$

$$Z_m = \begin{bmatrix} Z_{mx} & 0 \\ 0 & \end{bmatrix} \quad (29)$$

where: $Z_{mx} = Z_{my} = 4\,s + 0.04$ N/cm (30)

and $A_{fx} = -0.5$ and $A_{fy} = -1.5$ (31)

The elements of all weighting functions were chosen as $\frac{0.01}{s+1}$. Through the controller design procedure given in section 3, the controller was designed. Figures 8 shows the slave force and the master force along the X-direction. Figure 9 shows the slave force versus the master force where the slope of the fitted curve confirms the achievement of the desired force attenuation in the X-direction. Figures 10 and 11 are similar to figures 8 and 9 and show the force amplification along the Y-direction.

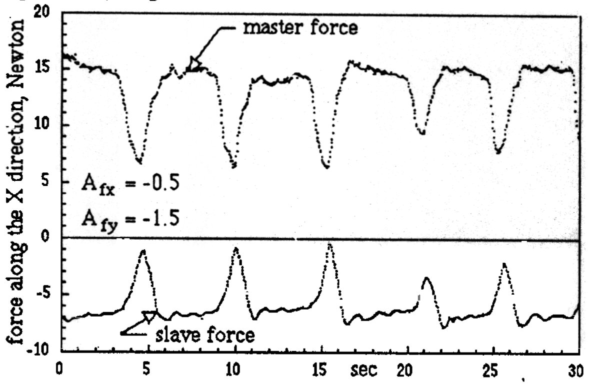

Figure 8: Plots of master and slave forces along the x-direction.

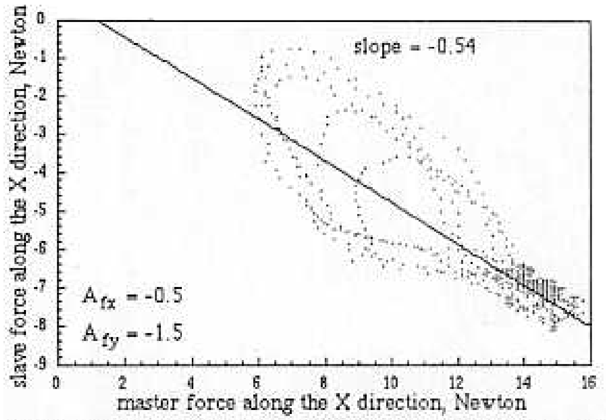

Figure 9: The slope of the fitted linear curve = - 0.54 confirms the force amplification of A_{fx} = - 0.5 along the x direction.

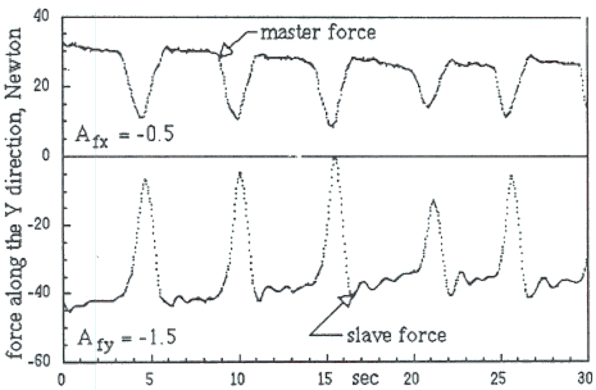

Figure 10: Plots of master and slave forces along the Y-direction.

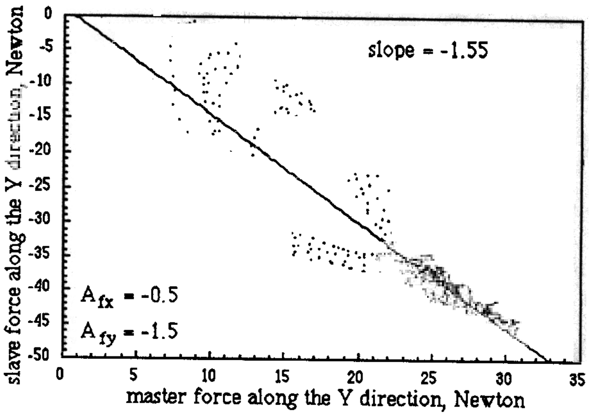

Figure 11: The slope of the fitted linear curve = - 1.55 confirms the force amplification of A_{fy} = - 1.5 along the y direction.

6. Summary and Conclusion

This paper presents a design framework for telerobotic systems to achieve desired dynamic relationships between the master robot and the slave robot. H_∞ control theory and model reduction techniques were used to guarantee that the system behavior was governed by the proposed specified functions. Several experiments were carried out to verify the theoretical derivations

7. References

1) Anderson, R. J., Spong, M. W., "Asymptotic Stability for Force Reflecting Teleoperators with Time Delay", IEEE Int. Conf. on Robotics and Automation, Scottsdale, AZ, May 1989.
2) Bejczy, A. K., Bekey, G., Lee, S. K., "Computer Control of Space Borne Teleoperators with Sensory Feedback", IEEE Conference on Robotics and Automation, 1985.
3) Doyle, J. C., Glover, K., Khargonekar, P., Francis, B. A., "State-Space Solutions to Standard H_2 and H_∞ Control Problems", IEEE Trans. on Aut. Control, V. 34. No. 8, 1989.
4) Francis, Bruce A., A Course in H_∞ Control Theory, Springer-Verlag, Berlin, 1987.
5) Glover, K.,"All Optimal Hankel-norm Approximations of Linear Multivariable Systems and Their L_∞ Error Bounds", International Journal of Control, Vol. 39, pp. 1115-1193, 1984.
6) Hannaford, B., "A Design Framework for Teleoperators with Kinematic Feedback", IEEE Transactions on Robotics and Automation, Vol. 5, No. 4, Aug. 1989.
7) Hannaford, B., "Stability and Performance Tradeoff in Bilateral Telemanipulations", IEEE Int. Conference on Robotics and Automation, Scottsdale, AZ, May 1989.
8) Kazerooni, H., "On the Robot Compliant Motion Control", ASME J. of Dyn. Systems, Measurement, and Control, Vol. 111, No. 3, Sep. 1989.
9) Kazerooni, H., Houpt, P. K., Sheridan, T. B., "Fundamentals of Robust Compliant Motion for Manipulators", IEEE Journal of Robotics and Automation, Vo'. 2, No. 2, Jun. 1986.
10) Kazerooni H., Kim S., "On the Design of Direct Drive Robots," ASME Journal of Engineering for Industry. Vol. 112, No. 2, May 1990.
11) Kazerooni, H., "On the Contact Instability of the Robots When Constrained by Rigid Environments," IEEE Transactions on Automatic Control, Volume 35, Number 6, June 1990.
12) Moore, B. C., "Principal Component Analysis in Linear System: Controllability, Observability and Model Reduction", IEEE Transactions on Automatic Control, AC-26, Feb. 1981.
13) Raju, G. J., Verghese, G. C., Sheridan, T. B., "Design Issues in Network Models of Bilateral Remote Manipulation", IEEE Int. Conf. on Robotics and Aut., Scottsdale, AZ, May 1989.
14) Stein, R. B., "What muscles variables does the nervous system control in limb movements?", J. of the Behavioral and Brain Sciences, Vol. 5, pp. 535-577, 1982.
15) Waibel, B. J., Kazerooni, H., "On the Stability of the Constrained Robotic Maneuvers in the Presence of Modeling Uncertainties," IEEE Transaction on Robotics and Automation, Vol. 7 No. 1. February 1991.